Imaging of epithelial tissue *in vivo* based on excitation of multiple endogenous nonlinear optical signals

Dong Li, Wei Zheng, and Jianan Y. Qu*

Department of Electronic and Computer Engineering, Hong Kong University of Science and Technology, Clear Water Bay, Kowloon, Hong Kong, China
**Corresponding author: eequ@ust.hk*

Received June 12, 2009; accepted July 19, 2009;
posted August 13, 2009 (Doc. ID 112748); published September 14, 2009

We demonstrate an integrated optical microscope to image the living epithelial tissue by simultaneously exciting multiple endogenous nonlinear optical signals. By employing the spectral lifetime detection capability, this technology provides a unique approach to sensing the fine structure, the protein distribution, and the cellular metabolism of epithelial tissue *in vivo*. In particular, we investigated the two-photon excitation fluorescence (TPEF) of tryptophan, an essential amino acid serving as the building block of protein. Our findings show that the TPEF of cellular tryptophan produces a good contrast to reveal the morphology of the epithelial cell layer, and the contrast can be further enhanced by applying low-concentration acetic acid.

OCIS codes: 180.4315, 320.6629, 170.6935, 180.6900, 170.6920, 170.3880.

Two-photon excitation fluorescence (TPEF) of endogenous fluorophores and second-harmonic generation (SHG) of structural proteins allow one to perform a noninvasive imaging of intact tissue with subcellular resolution. The reduced nicotinamide adenine dinucleotide (NADH) is considered as an endogenous fluorescence indicator of cellular metabolism. Because the concentration of NADH in mitochondria is much higher than other cellular compartments, the TPEF image of the NADH signal mainly reflects the distribution of mitochondria in cells [1,2]. The fluorescence of tryptophan, an essential amino acid involved in many important biochemical processes [3,4], conveys the information on the protein content and the microenvironment. In addition, the image of a tryptophan signal may reveal a clear cellular morphology because protein molecules distribute all over the cell. Finally, the signals of structural proteins (keratin, collagen, and elastin) can serve as the contrast agents for imaging the fine structure in the epithelial and the stromal layers [1,2]. Ideally, an imaging system to simultaneously excite multiple endogenous optical signals can provide more information on morphology and biochemistry of imaged tissue. However, the challenges are that the excitation and the emission wavelengths of these endogenous signals are generally different. Recently, we demonstrated a two-color two-photon excitation microscope to excite tryptophan and NADH fluorescence in living cells by using the supercontinuum generation from a photonic crystal fiber (PCF) [5]. In this Letter, an integrated two-photon excitation microscope is built to perform *in vivo* imaging of epithelial tissue.

The homebuilt two-photon microscope is similar to that reported in our previous study [5]. The PCF (NL-1.4-775, Crystal Fiber) was pumped by a femtosecond laser (Coherent, Mira-900) tuned at 760 nm. A portion of the pump laser and the filtered out supercontinuum at 600 ± 20 nm were used to excite the TPEF and the SHG signals simultaneously. The hamster cheek pouch was used as the living epithelial sample for *in vivo* imaging because it is a widely accepted model of human stratified squamous epithelium. The total power incident on the hamster oral tissue was less than 30 mW. After anaesthetization, the z-stack images were acquired with 16 s integration time for each optical sectioning depth, using 3 μm z-step size. The sampling area of each image was $90\ \mu\text{m} \times 90\ \mu\text{m}$ (128×128 pixels). A spectrograph equipped with a 16-channel photomultiplier tube (PMT) array and a time-correlated single-photon counting (TCSPC) module (PML-16 and SPC-150, Becker and Hickl BmbH) were used to record time-resolved TPEF and SHG signals from 310 to 510 nm with about a 13 nm resolution. This equipment allowed us to distinguish the fluorescence from different fluorophores based on their spectral and temporal characteristics.

Representative images measured from the hamster cheek pouch at different sectioning depths are displayed in Fig. 1. It is expected that the TPEFs in the wavelength region from 300 to 400 nm (U band) are determined by tryptophan fluorescence, which is excited by 600 ± 20 nm supercontinuum, whereas the major endogenous fluorophores with TPEF emissions in the 400–500 nm region (B band) are keratin, NADH, or extracellular matrix (ECM) proteins, which are excited by 760 nm laser light [6]. The TPEF intensity images formed in the B and the U bands are shown in the left and the middle columns in Fig. 1, respectively. The SHG images recorded from the stromal layer are presented together with corresponding TPEF images in Figs. 1(e3) and Fig. 1(f3), which is excited by 760 nm laser light. To separate the SHG excited at 760 nm from the TPEF in the U band, the excitation at 600 nm was delayed about 1 ns with respect to that at 760 nm. As can be seen, the TPEF images of stratum corneum (SC) in Figs. 1(a1) and 1(a2) are formed with bright and diffused pat-

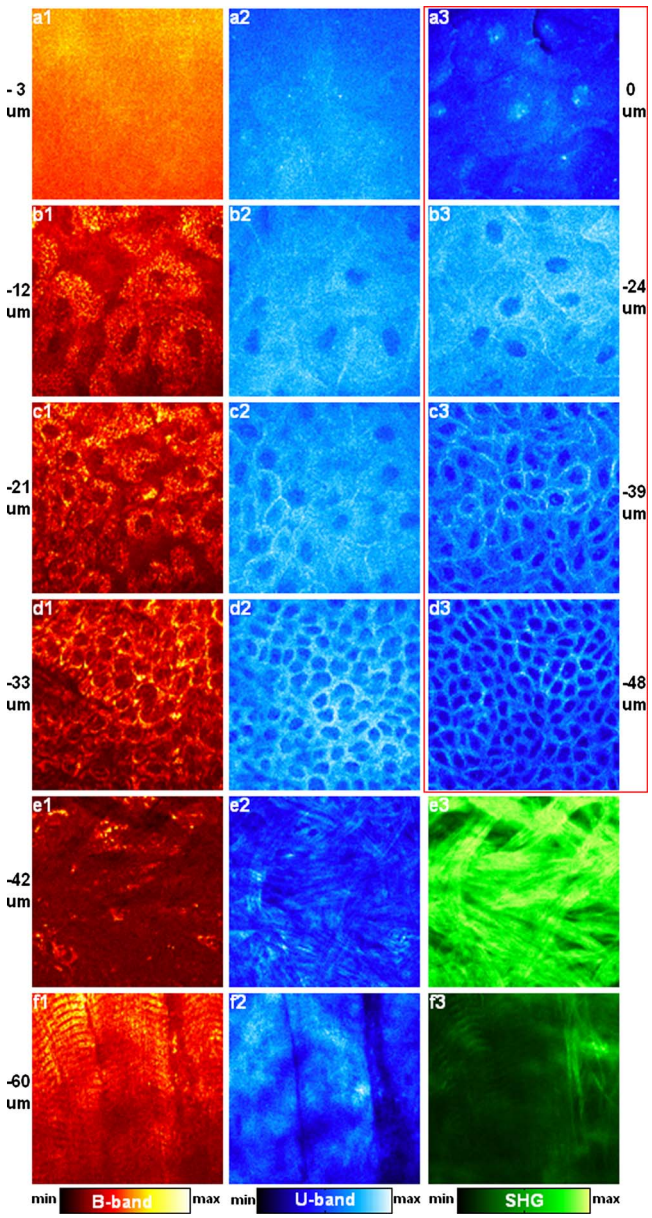

Fig. 1. (Color online) Representative TPEF and SHG images of hamster oral epithelium excited at 600 and 760 nm. *B* band, *U* band, and SHG images are presented in left, middle, and right columns, respectively: (a1)–(a3) SC; (b1)–(b3) SG; (c1)–(c3) stratum spinosum (SS); (d1), (d2) SB; (e1)–(e3) stroma (S); (f1)–(f3) soft muscle (M). (a3)–(d3) are *U*-band images of hamster cheek pouch exposed to 6% AA. Multimedia supplements: stack movies formed with the TPEF and SHG images simultaneously excited at 600 and 760 nm from tissues without (Media 1) and with (Media 2) 6% AA treatment. All images are reconstructed from raw data without any processing.

terns, indicating that the topmost epithelial layer is keratinized [7]. The images of the underlying nonkeratinized layer show that nuclear density increases from stratum granulosum (SG) down to stratum basale (SB). Particularly, the TPEF images in the *B* band from Figs. 1(b1) through 1(d1) are mainly characterized by the bright strips and spots of mitochondrial morphology. Unlike the *B*-band images, the distributions of signals in the *U* band are generally uniform in the cytoplasm and the nuclear compartments, respectively. The cellular morphology of nonkeratinized epithelium is clearly displayed in the *U*-band images shown in Figs. 1(b2) through 1(d2). The stromal layer can be identified by the SHG from collagen fibrillar bundles as shown in Fig. 1(e3). The patterns of relatively weak TPEF signals in stroma shown in Figs. 1(e1) and 1(e2) are correlated well with SHG, indicating that fluorescence in the *B* and *U* bands are from collagen fiber, too. In deeper optical sectioning depth, clear muscle structures are revealed by the SHG signals from myosin filaments and the *B*-band TPEF signals from the rest of the muscle fibers [8] shown in Figs. 1(f3) and 1(f1), respectively, while some bright patterns shown in the SHG image [Fig. 1(f3)] that are not correlated with muscle fibers are probably from collagen fibers. Clear muscle structures are not shown in the *U*-band image [Fig. 1(f2)], because tryptophan TPEF signals are from both myosin and the rest of the muscle fibers.

To investigate and verify the origins of observed fluorescence signals in the *U* and *B* bands, the spectral signals were measured from the SC, the epithelial cell, and the stromal layers with alternative excitations at 600 and 760 nm. The results are shown in Figs. 2(a) and 2(b). Each spectrum in the figures was the integration of signals over the sampling areas in a certain tissue layer. Comparing the TPEF spectrum of pure tryptophan with the TPEF signals of different tissue layers at 600 nm excitation, it is clear that the tryptophan fluorescence was dominant in the *U*-band TPEF signals of all tissue layers. At 760 nm excitation, strong keratin fluorescence that peaked around 490 nm was observed in the SC layer [6]. The signals from SG to SB were almost identical with a spectral peak at 450 nm. This confirms that NADH is the major fluorophore in nonkeratinized epithelium [2]. The stromal layer exhibited collagen that characterized a strong SHG signal and a fluorescence emission that peaked around 470 nm [6]. The SHG signal in stroma displayed in Fig. 2(b) was reduced by a factor of 200. The weak SHG signals shown in the spectrum of the SC and the epithelial layers were excited from the underlying stromal layer because of a thin hamster oral epithelium (~30 μm). The TPEF spectral signals of muscle fiber are almost identical to the epithe-

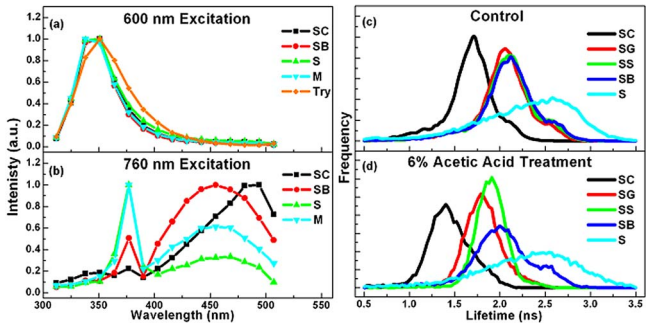

Fig. 2. (Color online) Representative TPEF spectra and lifetime histograms. (a) TPEF spectra excited at 600 nm from SC, SB, S, M, and tryptophan solution (Try); (b) corresponding spectra excited at 760 nm; (c) histograms of tryptophan fluorescence lifetime from SC, SG, SS, SB, and S layers without AA treatment; (d) corresponding histograms with 6% AA treatment.

lial layer, meaning that the signal sources of the *U* and the *B* band in muscle cells are tryptophan and NADH, respectively. The SHG signal in muscle displayed in Fig. 2(b) was reduced by a factor of 100.

It is known that NADH exists in free and protein-bound forms in living cells. The free/bound NADH ratio could be employed as an indicator for cellular metabolic status [9–11]. Similar to previous studies [5,11], we extracted free and bound NADH signals by using a dual exponential function to analyze the decay of the *B*-band TPEF measured from the nonkeratinized epithelial layers. It was found that the free/bound NADH ratio increased by (25±7)% from the SG to the SB layer, indicating a possible change in cellular metabolism throughout the epithelial layer. This change may be due to that epithelial cells become more mature and metabolically less active when grown upward from the basal layer [10].

Tryptophan fluorescence provides not only the information on protein distribution but also on microenvironmental changes around proteins. For example, the lifetime of tryptophan fluorescence is a sensitive indicator of pH value, because a low pH value could induce protein denaturation, fixation, and aggregation [12,13], which result in a decrease in tryptophan fluorescence lifetime [14]. Acetic acid (AA) is a widely used contrast agent for clinical diagnosis of cervical and skin precancers. In this study, we investigated whether AA-induced changes in tryptophan fluorescence could provide additional benefits and information for imaging of epithelial tissue. The oral epithelium of the live hamster was treated with 6% AA solution and the depth-resolved TPEF images were acquired about 1 min after the application of AA. Representative tryptophan fluorescence images recorded from the SC to the SB layer are shown in the third column of Fig. 1 from Figs. 1(a3) to 1(d3). Compared with the TPEF images of untreated epithelium, the contrast of the nucleus of dead cells to the surrounding cytoplasm in the SC and the contrast of the cell boundary and the nucleus to the cytoplasm in the underlying SG to the SB were obviously enhanced. The enhancements may be due to the interaction of AA with intracellular proteins and gap junction proteins. Detailed comparisons between the depth-resolved images recorded from the epithelial tissue before and after the AA treatment are shown in media 1 and 2. It was noted that the AA treatment caused a swelling of epithelial tissue by thickening the SC layer from 7±2 to 16±3 μm and the SG-SB layer from 25±4 to 30±5 μm. The AA-induced tissue swelling was also observed by other groups [15,16].

To monitor the penetration of AA in epithelial tissue, we analyzed the lifetimes of tryptophan fluorescence at different sectioning depths. The dual exponential function was used to analyze the fluorescence decay pixel by pixel in the tryptophan TPEF image recorded at certain depths. The lifetime histograms of tryptophan fluorescence calculated from the images recorded before and after the AA application are shown in Figs. 2(c) and 2(d), respectively. As can be seen from Fig. 2(c), the histograms of tryptophan fluorescence lifetimes in the SC, the SG-SB, and the stromal layers are significantly different, indicating that the protein compositions or profiles vary widely from tissue layer to layer. The lifetime distributions become shorter after the application of AA, meaning the decrease in pH values in all tissue layers [12]. This evidence demonstrates that AA penetrated throughout these tissue layers and the contrast enhancement of the cellular morphology in the tryptophan TPEF images may be induced by the interaction of AA with cellular proteins. In addition, the lifetime distributions of SG-SB layers are almost identical before the AA treatment. However, the distributions are clearly separated after the application AA. The results provide qualitative information on the gradient of the pH value or the AA concentration in the epithelial layer.

This work is supported by the Hong Kong Research Grants Council through grant HKUST618808.

References

1. W. R. Zipfel, R. M. Williams, R. Christie, A. Y. Nikitin, B. T. Hyman, and W. W. Webb, Proc. Natl. Acad. Sci. USA **100**, 7075 (2003).
2. L. H. Laiho, S. Pelet, T. M. Hancewicz, P. D. Kaplan, and P. T. C. So, J. Biomed. Opt. **10**, 024016 (2005).
3. J. D. Schaechter and R. J. Wurtman, Brain Res. **532**, 203 (1990).
4. P. Diagaradjane, M. A. Yaseen, J. Yu, M. S. Wong, and B. Anvari, Lasers Surg. Med. **37**, 382 (2005).
5. D. Li, W. Zheng, and J. Y. Qu, Opt. Lett. **34**, 202 (2009).
6. Y. Wu and J. Y. Qu, Opt. Lett. **30**, 3045 (2005).
7. M. C. Skala, J. M. Squirrell, K. M. Vrotsos, J. C. Eickoff, A. G. Fitzpatrick, K. W. Eliceiri, and N. Ramanujam, Cancer Res. **65**, 1180 (2005).
8. C. Odin, T. Guilbert, A. Alkilani, O. P. Boryskina, V. Fleury, and Y. L. Grand, Opt. Express **16**, 16151 (2008).
9. D. K. Bird, L. Yan, K. M. Vrotsos, K. W. Eliceiri, E. M. Vaughan, P. J. Keely, J. G. White, and N. Ramanujam, Cancer Res. **65**, 8766 (2005).
10. M. C. Skala, K. M. Riching, A. G. Fitzpatrick, J. Eickhoff, K. W. Eliceiri, J. G. White, and N. Ramanujam, Proc. Natl. Acad. Sci. USA **104**, 19494 (2007).
11. D. Li, W. Zheng, and J. Y. Qu, Opt. Lett. **33**, 2365 (2008).
12. A. B. MacLean, Gynecol. Oncol. **95**, 691 (2004).
13. A. Hickel, M. Graupner, D. Lehner, A. Hermetter, O. Glatter, and H. Griengl, Enzyme Microb. Technol. **21**, 361 (1997).
14. E. Gudgin, R. L. Delgado, and W. R. Ware, Can. J. Chem. **59**, 1037 (1981).
15. T. Collier, P. Shen, B. Pradier, K. B. Sung, R. R. Kortum, A. Malpica, and M. Follen, Opt. Express **6**, 40 (2000).
16. S. P. Tai, W. J. Lee, D. B. Shieh, P. C. Wu, H. Y. Huang, C. H. Yu, and C. K. Sun, Opt. Express **14**, 6178 (2006).